PHYSICS OF PLASMAS 24, 103510 (2017)

Electrical model of cold atmospheric plasma gun

Ya. Z. Slutsker,[1] V. E. Semenov,[2] Ya. E. Krasik,[1] M. A. Ryzhkov,[1] J. Felsteiner,[1]
Y. Binenbaum,[3] Z. Gil,[3,4] R. Shtrichman,[3] and J. T. Cohen[3,4]
[1]*Physics Department, Technion-Israel Institute of Technology, Haifa 32000, Israel*
[2]*Institute of Applied Physics, RAS, Nizhny Novgorod 603950, Russia*
[3]*Laboratory of Applied Cancer Research, Rambam Healthcare Campus, Haifa, Israel*
[4]*Rappaport Faculty of Medicine, Technion-Israel Institute of Technology, Haifa, Israel*

(Received 31 May 2017; accepted 4 September 2017; published online 26 September 2017)

We present an analytical model of cold atmospheric plasma formed by a dielectric barrier discharge (DBD), which is based on the lumped and distributed elements of an equivalent electric circuit of this plasma. This model is applicable for a wide range of frequencies and amplitudes of the applied voltage pulses, no matter whether or not the generated plasma plume interacts with a target. The model allows quantitative estimation of the plasma plume length and the energy delivered to the plasma. Also, the results of this model can be used for the design of DBD guns which efficiently generate cold atmospheric plasma. A comparison of the results of the model with those obtained in experiments shows a fairly good agreement. *Published by AIP Publishing.*
[http://dx.doi.org/10.1063/1.4986023]

I. INTRODUCTION

The subject of cold atmospheric plasma (CAP) application for medicine, especially for cancer treatment, has attracted large attention due to the promising results obtained. The number of publications on this subject has grown very rapidly, reaching hundreds during the last few years[1] and already in 2012, the total number of papers related to CAP reached 20 000.[2] Results of this research, carried out in several laboratories and scientific centers around the world, are summarized in several review papers[1–14] and a text book.[15]

In most studies, CAP is formed as a result of dielectric barrier discharge (DBD) by application of a high-voltage (HV) single pulse having duration of tens of nanoseconds or HV pulses applied with the repetition rate in the range 10^3–10^6 Hz, voltage amplitude in the range 2×10^3–4×10^4 V, and discharge current ≤ 10 mA.[15,16] Different types of gases (He, Ar, Xe, and air) with different flow rates (1–12 l/min) were used for the plasma formation.

Parameters of the plasma were studied using optical, spectroscopic and microwave methods and using electrical probes. It was shown that formation of the CAP is accompanied by generation of excited states of neutrals, ions, and hydroxyl radicals. It was shown that in the case of application of the HV pulses with frequency of several tens of kHz, the plasma formation occurs as a single elementary discharge during the oscillation period. At present, it is well accepted that this plasma can be considered as highly collisional and not in thermal equilibrium. Depending on the frequency and amplitude of the HV pulses and the type of the gas and its flow rate, the plasma electron density was found in the range 10^{12}–10^{13} cm^{-3} (ionization level $\leq 10^{-6}$) with the temperature of the neutral gas in the range 300–350 K.

Formation of the DBD discharge inside a dielectric tube leads to the formation of a plasma jet with length up to 10 cm outside the dielectric tube. It was also suggested that the propagation of this current carrying plasma jet ($\sim$1 mA) can be explained by a streamer phenomenon and that due to the rather good conductivity of the streamer channel ($\leq 10^{-2}\,\Omega^{-1}$ cm^{-1}), almost all the potential of the electrodes is transferred to the streamer tip. The velocity of the streamer propagation was measured as $\leq 10^8$ cm/s (depending on parameters of the discharge) with electric field in the streamer channel being $\sim$100 V/cm to $\sim 10^5$ V/cm at the vicinity of the streamer tip.

In the case when the output of the dielectric tube was connected to a dielectric elastic capillary, plasma bullets were formed which could be transported along distances ≥ 1 m. The latter led to the suggestion that these plasma bullets can be transported within the human body to a desired location. The formation of CAP and plasma bullets were studied applying 1D and 2D numerical simulations (see, for instance, Refs. 17–20) taking into account many excitation and ionization processes involved in the plasma formation and propagation. These numerical studies show that plasma bullets propagate in the form of fast ionization waves forming electric field and charged and excited particles at remote locations and the bullet structure and propagation velocity depend on the geometry of the dielectric channel.

However, numerical modeling of the CAP generation in some specific geometry of the plasma gun cannot be used for prediction of the plasma parameters in the case of a change in the parameters of the discharge (geometry, rf voltage amplitude, gas flow rate, frequency, gas type, etc.). Therefore, analytical modeling is strongly required. Such modeling allows one to understand the main phenomena involved in the CAP generation and to predict the plasma characteristics in the case of the change in the discharge parameters.

In this paper, we present an analytical model which allows one to explain and predict the CAP parameters such as the power delivered to the plasma, plasma plume length versus the driving voltage and driving frequency, distance to the target, etc. The results of this model were compared with results obtained with a CAP plasma gun working in a

Penning gas mixture at reduced rf voltage amplitude and gas flow rate.[21]

II. SIMPLIFIED ANALYTICAL MODEL OF THE CAP GENERATION

First, we note that the major part of the experimental research of CAP generation was carried out using HV single pulses with duration of 10^{-8}–10^{-6} s applied with a repetition rate up to 10^3 Hz or using RF pulses with a frequency $<10^4$ Hz. Under these conditions, the plasma discharge was ignited and terminated during each single pulse or was ignited twice within the period of the applied voltage oscillation. Therefore, in the modeling, the main attention was related to the non-stationary process of the discharge development during the rise/fall times of the single voltage pulse or during the half-period of the ac voltage. The main disadvantage of this approach of the CAP generation is the necessity of the voltage amplitude, required for the gas breakdown, to be significantly larger than the amplitude of the voltage necessary to keep a quasi-stationary discharge.[22]

This disadvantage can be avoided by the application of voltage pulses with high frequency ($>10^6$ Hz) and by the use of special gas mixtures such as Penning gas (98%–99.5% of Ne and 0.5%–2% of Ar).[21] At these conditions, significantly smaller amplitude of the breakdown voltage is required than in the case of pure noble gases. Application of high frequency electric field also simplifies the modeling of the discharge. Indeed, in this case, the period of the electric field becomes smaller than the plasma relaxation time. The latter allows one to neglect the plasma density modulations and to develop a quasi-stationary model of the plasma discharge. Using this model, one can make estimations of the electric field in the plasma and the power delivered to the plasma using the simple impedance scheme shown in Fig. 1. If one applies to the input of this scheme an ac voltage with frequency ω and amplitude U_0, in this case, the complex amplitudes of the current and voltage on the plasma load and the power delivered to the plasma are $I = U_0/(Z_c + Z_p), U_p = U_0 Z_p/(Z_c + Z_p)$ and $P_p = 0.5\mathrm{Re}(U_p^2/Z_p)$, respectively. Thus, in order to obtain the main plasma characteristics, one should determine the coupling Z_c and plasma Z_p impedances and it is not necessary to know the evolution of the plasma during the electric field oscillation period.

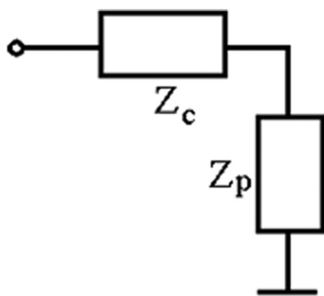

FIG. 1. Electrical scheme for the calculation of the energy deposited in a quasi-stationary plasma. The complex coupling impedance $Z_c(\omega)$ is determined by the system geometry. The complex impedance of the plasma $Z_p(\omega)$ depends on the plasma density and the dimensions of the plasma occupied volume.

We will consider two models related to the plasma plume with and without its interaction with a target. In the case when the plasma plume interacts with a target, the plasma is localized in a small volume between the plasma gun output and the target and one can analyze the plasma parameters using non-distributed, discrete electric circuit elements. In this approach, the plasma generation will be considered during low-frequency and high-frequency voltage pulses.

A. Low-frequency high-voltage pulses

The model considers the electrical scheme shown in Fig. 2 for CAP generation by a DBD discharge.[23] The voltage U is applied to two capacitors connected in series. The capacitor C_d consists of the HV electrode and the dielectric layer covering this electrode. The voltage drop on this capacitor is U_d. This capacitor couples the rf power supply and the gas-filled discharge gap represented by the capacitor C_g with the voltage drop U_g. However, when the plasma is generated in this gap, the capacitor C_g becomes shorted by the plasma non-linear resistance R_g, whose value changes in time in inverse proportion to the plasma density, n_p^{-1}. The temporal evolution of the voltages $[U(t), U_d(t), U_g(t)]$ and the current $I(t)$ in this electrical scheme can be described by a system of ordinary differential equations

$$I = C_d \frac{dU_d}{dt} = C_g \frac{dU_g}{dt} + \frac{U_g}{R_g},$$
$$U_d + U_g = U(t). \tag{1}$$

To solve Eq. (1) for a known $U(t)$, one should consider the dependence of the resistance R_g on U_g and I. In the model of low-frequency gas discharge,[24] the ionization and recombination times in the plasma were considered to be shorter than the period of the applied voltage. Thus, the value of n_p increases with the increase in the electric field E_g in the plasma. In this case, one can use the approximation for the non-linear dependence of R_g on U_g and I

$$R_g = \infty, \text{ if } |U_g| < U_p, \tag{2}$$
$$|U_g| = U_p = \text{const, if } R_g < \infty, \tag{3}$$

where U_p is the voltage drop on the gas gap which is necessary to sustain the discharge. For a known applied voltage $U(t) = U_0 \cos(\omega t)$, one obtains from Eq. (1)

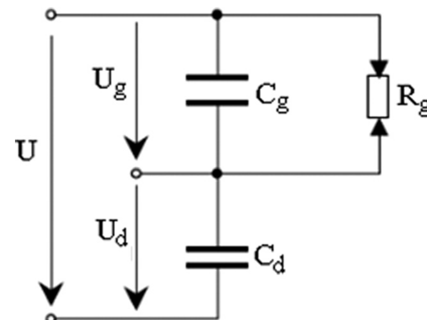

FIG. 2. Electrical scheme of the model.

$$I = C_d \frac{dU_d}{dt} = C_d \frac{dU}{dt}. \quad (4)$$

One can see that when U reaches its maximal value, i.e., $dU/dt = 0$, the current becomes equal to zero and the gas discharge is terminated. The solution of Eq. (1) also becomes periodic in time. In the case when the gas gap voltage is $|U_g(t)| = U(t)C_d/(C_d + C_g) < U_p$, the gas discharge is not realized, $R_g = \infty$ and the solution of Eq. (1) is

$$U_g(t) = C_d U_0 \cos(\omega t)/(C_d + C_g),$$
$$I(t) = -C_d C_g \omega U_0 \sin(\omega t)/(C_d + C_g). \quad (5)$$

However, when the gap voltage U_g becomes sufficient for the gas breakdown, i.e., $|U_g| \geq U_p$, one obtains gas discharge accompanied by plasma generation. According to Eq. (4), the plasma discharge is terminated at $t = 0$ corresponding to the maximal value of the applied voltage. This condition allows one to find the solution of Eq. (1) during the period of the voltage oscillation. Indeed, at $t = 0$, one obtains $I = 0$, $U_g = U_p, U_d = U_0 - U_p$ and during some certain time at $t > 0$, there is no plasma in the gas-filled gap. Thus, using conditions for current and voltages at $t = 0$, the solution of Eq. (1) reads

$$U_g(t) = U_p - 2C_d U_0 \sin^2(0.5\omega t)/(C_d + C_g),$$
$$I(t) = -C_d C_g \omega U_0 \sin(\omega t)/(C_d + C_g). \quad (6)$$

At the time when the voltage on the gas-filled gap reaches the value $-U_p$, the ignition of the gas discharge will be realized and up to the time $t = \pi/\omega$, the solution of Eq. (1) will be

$$U_g = U_p, \quad I = -C_d \omega U_0. \quad (7)$$

In half the period, $t = \pi/\omega$, the current in the discharge gap once more approaches zero and the discharge is terminated. Further at $t > \pi/\omega$, this cycle will be repeated but in an antisymmetric form, i.e., at the first stage, when $U_g < U_p$

$$U_g(t) = -U_p + 2C_d U_0 \sin^2(0.5\omega t)/(C_d + C_g),$$
$$I(t) = -C_d C_g \omega U_0 \sin(\omega t)/(C_d + C_g), \quad (8)$$

and later in time up to $t = 2\pi/\omega$

$$U_g = U_p, \quad I = -C_d \omega U_0 \sin(\omega t). \quad (9)$$

Now, using the known voltage drop on the discharge plasma gap and the current flowing through the plasma, one can calculate the average power deposited in the discharge plasma

$$\langle Q \rangle = (2\omega/\pi) C_d U_p \left[U_0 - (C_d + C_g)U_p/C_d\right]. \quad (10)$$

To summarize this part, we note that the application of low-frequency HV pulses for CAP generation corresponds to the major part of the experimental research carried out so far.

B. High-frequency high-voltage pulses

Next, we consider the case of high-frequency plasma discharge when the change in the plasma density is insignificant during the discharge, i.e., $R_g = \text{const}$. In this case, the current and the voltage drop on each element of this scheme also vary according to the harmonic law. The latter allows one to apply the method of impedances for dielectric capacitor $Z_c = (i\omega C_d)^{-1}$ and plasma $Z_p = R_g/(1 + i\omega C_g R_g)$ to determine the parameters of the circuits shown in Figs. 1 and 2. In this case, the amplitude of the voltage on the gas gap and the average deposited power in the plasma due to Ohmic heating are

$$U_{go} = U_0 \omega C_d R_g \left[1 + \omega^2 R_g^2 (C_d + C_g)^2\right]^{1/2},$$
$$Q = 0.5 U_{go}^2 / R_g. \quad (11)$$

In the general case, the resistance of the gas-filled gap is not a linear function and it depends on U_{g0}. Similar to the case of low-frequency voltage pulses, one can consider a step-function dependence[25] for this resistance

$$R_g = \infty, \ \text{if } U_{g0} < U_s, \quad (12)$$

$$U_{g0} = U_s, \ \text{if } R_g < \infty, \quad (13)$$

where U_s is the amplitude of the voltage which is necessary to keep the plasma discharge. Using this approximation, the gas discharge will be realized when $U_0 > U_s(C_d + C_g)/C_d$, and the average power dissipated in the plasma due to Ohmic heating will be

$$Q = 0.5 U_s \omega C_d \left\{U_0^2 - \left[(C_d + C_g)/C_d\right]^2 U_s^2\right\}^{0.5}. \quad (14)$$

This model allows one to determine the difference between the threshold voltage U_b required for the plasma discharge initiation and the value of U_s by changing conditions (12) and (13) as

$$R_g = \infty, \ \text{if } U_{g0} < U_b, \quad (15)$$

$$U_{g0} = U_s, \ \text{if } R_g < \infty. \quad (16)$$

In this case, for the plasma discharge initiation, one requires $U_0 > (C_d + C_g)U_b/C_d$. However, after the discharge initiation, one can keep this discharge by decreasing the amplitude of the applied voltage to the value $U_0 = (C_d + C_g)U_s/C_d$. The average power dissipated in the discharge will be determined by the same Eq. (14). Also, using Eq. (14) and the values of Q, U_s and U_b measured in the experiment, the values of $(C_d + C_g)U_s/C_d$ and $(C_d + C_g)U_b/C_d$ can be determined. This model corresponds to the experimental conditions as realized in the experiments described in Ref. 21.

C. Plasma plume without the interaction with a target

CAP generation without a target placed at some distance with respect to the plasma gun output is accompanied by the formation of a cylindrical plasma plume at the output of the plasma gun.[2,3,11,20,26,27] This plasma plume is characterized by the length which significantly exceeds its diameter. The plume formation was considered as a non-stationary process of the streamer time and space evolution during an applied short-duration voltage pulse. Numerical modeling of this

process was based on the solution of electrostatic equations and hydrodynamic motion of charged particles accounting for their drift in electric field, diffusion processes, electron impact ionization, attachment and electron-ion recombination processes.[28] The qualitative model of the plasma plume formation based on the electrical scheme shown in Fig. 3 (here capacitors C_i and variable resistors R_i describe plasma elementary parts per unit length, respectively) was considered in Ref. 29. Using this scheme, a simple diffusion equation describing the electrodynamic evolution of the plasma plume was used:

$$\frac{\partial F}{\partial t} = \frac{\partial}{\partial z}\left(D\frac{\partial F}{\partial z}\right), \tag{17}$$

where the function $F(z,t)$ describes instantaneous distribution of the electric potential along the plasma plume where the diffusion coefficient $D = (\tilde{c}\rho)^{-1}$ is determined by the capacitance $\tilde{c}$ and resistance ρ per unit length.

In the case of high-frequency HV pulses, one can consider formation of a steady state plasma in which the plasma plume can be treated as a plasma column. The main objectives of the modeling are to determine the dependence of the plasma parameters on the voltage amplitude, geometry of the plasma gun, and properties of the surrounding media. The latter is important for medical applications when plasma should be delivered inside the human body through a dielectric tube.

Formation of a steady state plasma column is possible only if a sufficiently strong electric field exists inside the plasma. The latter can be realized for a surface electromagnetic wave propagating along the plasma column. In fact, the formation of a cylindrical plasma by a propagating surface electromagnetic wave which also sustains plasma is a well-known phenomenon studied in a broad range of frequencies 10^7–10^9 Hz at different pressures and types of gas.[30]

Thus, let us consider a surface electromagnetic wave propagating along the plasma column. Also, let us consider that the electromagnetic wave length is significantly smaller than its "vacuum" length but it is significantly larger than the typical diameter of the plasma column. The first condition indicates strong slowdown of the wave and allows one to use a quasi-electrostatic description of the electromagnetic field. The second condition allows one to consider the quasi-uniformity of the electromagnetic wave amplitude in the cross-sectional area of the plasma column. Also, in the case of normal atmospheric pressure, the radial uniformity of the electric field is a necessary condition for obtaining a uniform plasma density radial distribution. Within the frame of the quasi-electrostatic model, the complex amplitude of the electric field is

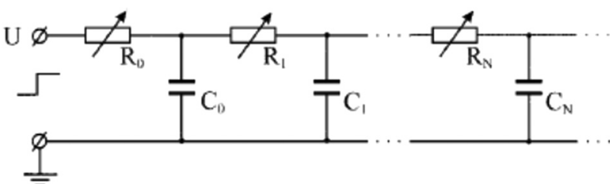

FIG. 3. Electrical scheme of the plasma plume formation.

$$\vec{E} = -\nabla\varphi, \quad \nabla(\varepsilon\nabla\varphi) = 0, \tag{18}$$

where ϕ is the complex amplitude of the electric potential, $\varepsilon = 1 - (1 + i\nu\omega^{-1})\omega_p^2(\omega^2 + \nu^2)^{-1}$ is the plasma complex dielectric permittivity, ω_p is the plasma electron frequency ($\omega_p^2 = 4\pi e^2 n_p/m$), ω is the electromagnetic wave frequency, and ν is the effective collision frequency of electrons with molecules. At atmospheric pressure $\nu \approx 2$–$4 \times 10^{12}\,\mathrm{s}^{-1}$ and for $\omega \approx 10^7\,\mathrm{s}^{-1}$, one obtains $\nu \gg \omega$ and, respectively, $\varepsilon \cong 1 - i\frac{\omega_p^2}{\omega\nu}$. The solution of Eq. (18) for a travelling electromagnetic wave with axial symmetry is

$$\varphi = \Phi(r)\cdot\exp(-ikz), \tag{19}$$

where k is the complex wave number describing propagation and damping of this wave. The potential radial distribution inside and outside of the plasma column is described by the Bessel equation

$$\frac{1}{r}\frac{d}{dr}\left(r\frac{d\Phi}{dr}\right) - k^2\Phi = 0. \tag{20}$$

Inside a plasma column with radius a, the solution of Eq. (20) reads

$$\Phi(r) = \Phi_0 I(kr), \tag{21}$$

where Φ_0 is the complex amplitude of the potential at the axis of the plasma column and I_0 is the modified Bessel function of the first kind. Outside of the plasma column, the solution of Eq. (20) is described by K_0, the modified Bessel function of the second kind

$$\Phi(r) = AK_0(kr). \tag{22}$$

The constant A on the right side of Eq. (22) and the wave vector k can be derived from the boundary conditions due to the continuity of the tangential component of the electric field and the normal component of the electric displacement

$$\begin{aligned} \Phi_0 I_0(ka) &= AK_0(ka), \\ \varepsilon\Phi_0 I_0'(ka) &= AK_0'(ka). \end{aligned} \tag{23}$$

In the case when $|ka| \ll 1$, the normal component of the electric field inside the plasma column is significantly smaller than the tangential component which is almost constant along the radius $[I_0(kr) \cong 1 + (kr)^2/4]$. In this case, an approximate solution of Eq. (23), which is a dispersion equation, can be written as

$$2/\varepsilon \cong (ka)^2[\ln(ka/2) + \gamma] \approx -(ka)^2\ln(1/|ka|), \tag{24}$$

where $\gamma \cong 0.577$ is the Euler number. One can see that the condition $|ka| \ll 1$ is satisfied for a rather dense plasma when $|\varepsilon| \gg 1$ i.e., the dielectric permittivity consists mainly of its imaginary part $\varepsilon \cong 4\pi\sigma(i\omega)^{-1}$ where $\sigma = e^2 n_p/m\nu$ is the plasma conductivity. Thus, the moduli of imaginary and real parts of the wave number are approximately equal to each other $|k'| \cong |k''| \cong |k|/\sqrt{2}$. The latter corresponds to the condition of equality between the energy dissipated in the elementary resistor and the energy stored in the elementary capacitor during the

process of its charging (see Fig. 3). In the first approximation, the imaginary part of the wave vector k'', which is responsible for the wave damping, can be associated with the plasma column length $L \approx 1/|k''| \cong \sqrt{2}/|k|$. Indeed, at larger distances, the electric field can be insufficient to sustain the plasma because of the wave absorption. Using Eq. (24), one can obtain the relation between the length L and the conductivity σ of the plasma column as: $\sigma \approx (\omega/4\pi)(L/a)^2 \ln^{-1}(L/a)$.

In the case of a plasma column with radius a, length L, and conductivity σ, we have $\tilde{c} = 0.5/\ln(L/a)$ and $\rho = 1/(\pi a^2 \sigma)$. Using these parameters, the diffusion equation (17) can be represented as a dispersion equation:

$$i\omega + k^2 2\pi a^2 \sigma \ln(L/a) = 0, \tag{25}$$

which is an approximation of Eq. (24). It should be noted that the applicability of the diffusion equation (17) is wider than that of a dispersion equation. In particular, Eq. (17) may be used to study plasma columns whose parameters are not uniform along the plasma length.

In the case of a monochromatic electric field, Eq. (17) can be solved using the method of complex amplitudes which may transform it to

$$i\omega E(z) = \frac{\partial^2}{\partial z^2}\{D(z)E(z)\}, \tag{26}$$

where $E(z) = \partial F/\partial z$ is the complex amplitude of the longitudinal electric field in the plasma. Approximating the electric field amplitude $|E|$ as constant along the plasma column, one can find the axial distribution of the diffusion coefficient[24] and the complex amplitude of the electric field as

$$D = \frac{\omega}{3}(z - z_0)^2, \quad E = E_s \exp\left\{2i\ln\left(\frac{z - z_0}{z_0}\right)\right\}, \tag{27}$$

where $z < z_0$, z_0 is the plasma column boundary and E_s is the electric field amplitude necessary to sustain plasma discharge. Equation (27) can be related to the plasma parameters using $D = 2\pi a^2 \sigma \ln(L/a)$. It should be noted that close to the plasma column boundary z_0, the diffusion coefficient approaches zero that corresponds to the plasma conductivity also approaching zero, and therefore, the mentioned above inequality, $|\varepsilon| \gg 1$, is violated. Thus, in this location, Eq. (27) is not valid. However, in the case when the length of the plasma column is much larger than the column diameter, Eq. (26) and its solution (27) are valid for almost all the length of the plasma column.

The relation of the plasma parameters to the plasma gun design can be found if the input impedance of the plasma column and the applied voltage are known as a function of the plasma column length. The necessary functions can be determined based on Eq. (17) and its solution (27). Specifically, the applied voltage is

$$F_p = \frac{4L}{3(1+i)} E_s. \tag{28}$$

The plasma column impedance is the ratio between the complex amplitudes of the potential and current $J = \pi a^2 \sigma E$

$$Z_p = \frac{8}{(1+i)L} \frac{\ln(L/a)}{\omega}. \tag{29}$$

Z_p is the complex impedance shown in Fig. 1. For instance, using the coupling impedance as the impedance of the capacitor C_d (also shown in Fig. 1), $Z_c = (i\omega C_d)^{-1}$, one can determine the voltage drop on the plasma column

$$|U_p| = \frac{U_0}{1 + |Z_c/Z_p|} = U_0 \left| \frac{iC_d 8\ln(L/a)}{iC_d 8\ln(L/a) + L(1+i)} \right| = U_0 \frac{C_d 8\ln(L/a)}{\sqrt{L^2 + (L + C_d 8\ln(L/a))^2}}. \tag{30}$$

But, the value of $|U_p|$ is equal to the potential at the input of the plasma column, i.e., $|U_p| = |F_p|$. Using this equality together with Eqs. (29) and (30) and the axial distribution of the plasma conductivity $\sigma = (\omega/6\pi)[(z - z_0)/a]^2 \ln^{-1}(L/a)$ [(see Eq. (27)], one can obtain the parameters of the plasma column for known values of U_0, E_s, a, ω, C_d. In the case of a rather short plasma column

$$L \ll 8C_d \ln(L/a), \tag{31}$$

the plasma impedance is larger than the coupling impedance of the dielectric capacitor, ($|Z_p| \gg |Z_c|$) and almost all the voltage is applied to the plasma, ($|U_p| \cong U_0$). The latter leads to an increase in the plasma length proportional to the applied voltage, $L \approx U_0/E_s$. In the opposite case, i.e., large length of the plasma column when $L \gg 8C_d \ln(L/a)$, the plasma impedance is small ($|Z_p| \ll |Z_c|$), and therefore, almost all the voltage is applied to the capacitor ($|U_p| \ll U_0$) and the plasma column length increases as

$$L \approx \left[(U_0/E_s) 6C_d \ln(L/a)\right]^{1/2}. \tag{32}$$

The energy density deposited into the plasma $q = 0.5\sigma E_s^2$ decreases along the plasma column and the total power deposited into the plasma is

$$Q \approx 0.06\omega E_s^2 L^3 \ln^{-1}(L/a). \tag{33}$$

It is understood that the total power deposited into the plasma [see Eqs. (10), (14) and (33)] is the most crucial parameter which determines the efficiency of the processes of the plasma interaction with a biological object and its average value can be measured in experiments.[21]

Finally, it should be noted that the electromagnetic field of the surface wave propagating along the plasma column is not completely localized inside the plasma. As can be seen from Eqs. (22) and (23), the longitudinal component of the rf electric field amplitude is the same inside and outside the plasma in the vicinity of the column boundary. However, the transverse component of the electric field is significantly larger outside the plasma than inside the plasma when the plasma density is high enough (when $|\varepsilon| \gg 1$). The latter means that the flux of the electromagnetic energy of the surface wave is localized mainly outside the plasma column and possible absorption of electromagnetic energy in the surrounding medium can play a crucial role in the surface wave damping.

For instance, in the case when the plasma column is located inside the dielectric tube which is surrounded by a medium with relatively high conductivity, the electric field can be considerably suppressed inside this medium. As a result, the longitudinal component of the electric field will be close to zero at the outside boundary of the dielectric tube. Within such an approximation (zero value of the longitudinal component of the electric field at the boundary of the conductive environment), the solution of Eq. (20) inside the dielectric tube becomes different from that given in Eq. (22). This solution can be represented as follows:

$$\Phi(r) = A\ln(r/b), \tag{34}$$

where b is the external radius of the dielectric tube. Using continuity of the tangential and normal components of the electric field and the electric displacement at the plasma boundary, one can find the dispersion equation to be different from Eq. (24)

$$(ka)^2 \cong -\frac{2\varepsilon_d}{\varepsilon\ln(b/a)}, \tag{35}$$

where ε_d is the dielectric constant of the dielectric tube material. It can be shown that under these conditions, in Eqs. (24)–(33) instead of $\ln(L/a)$, one has to use $\ln(b/a)/\varepsilon_d$ which is 5–10 times smaller. Thus, the length of the plasma plume can be considerably reduced when the latter penetrates into a conducting medium such as a biological object.

One can also consider another simple qualitative explanation for the decrease in the plasma plume propagation inside the dielectric tube surrounded by conductive environment. Indeed, in this condition, the stray capacitance between the plasma and the environment increases significantly. The latter decreases the voltage drop on the plasma and, respectively, will terminate the plasma generation and its propagation inside the dielectric tube.[18,19]

III. COMPARISON BETWEEN EXPERIMENTAL DATA AND THE MODEL RESULTS

As it was mentioned in the Introduction, the major part of CAP research was carried out using low-frequency HV pulses. However, the application of sinusoidal high-frequency (MHz range) voltage pulses has advantages related to enhanced safety, higher efficiency of the plasma gun operation and low voltage threshold for the DVD plasma generation.[21] This type of plasma gun operation was realized in our research and the average power delivered to the plasma will be compared with its value calculated using the developed model.

The experimental setup and its general view are shown in Figs. 4(a) and 4(b), respectively. The setup consists of gas distribution system, rf generator, and rf coaxial cable connected to the plasma gun.[21] The generator produces rf pulses with carrier frequency and voltage in the range 1.5–1.6 MHz and 850–1400 V, respectively. The duration and the repetition rate of the rf pulses were varied in the range 400–800 μs and 150–600 Hz, respectively. This range of the rf pulse parameters allows one to change in a wide range the power (0.1–5 W) deposited in the CAP, remotely measured with a meter installed in the rf generator. The rf power delivered to the plasma was measured using a power meter built-in the electronic scheme of the rf generator. The power meter was calibrated with a set of low-inductance precise resistors which were used as different loads, thus imitating the plasma gun operation at different parameters of the voltage amplitude, repetition rate, and rf pulse duration. The voltage waveform across these resistors was measured using a Tektronix high-voltage divider having high ($\sim$100 MΩ) input resistance and low input capacitance ($\sim$3 pF), which is smaller than the capacitance of the rf cable ($\cong$110 pF). The average power was calculated using the measured voltage waveform and the known values of the resistance and the repetition rate. This calibration was carried out for the whole range of rf power used in our research for cancer treatment. The error in the rf power meter calibration was estimated as $\pm$5%.

The plasma gun consisted of a PYREX tube having 6 mm outer and 4 mm inner diameters with the tube length being $\sim$40 mm. A ring-type rf electrode with outer insulation made of epoxy glue was placed close to the tube opening. The gas flow rate though the tube was varied in the range 0.5–5 l/min. A grounded target, made of 0.2 mm thick copper foil, was placed at different distances, 0.2–5 cm, with respect to the plasma gun output. A gas breakdown occurred when the rf voltage U_o, applied to the plasma gun, exceeded $U_b = 725 \pm 25$ V. The minimal repetition rate was found to be 150 Hz; at smaller repetition rates, the threshold voltage increased.

The experimental results showed that independently of the position of the target with respect to the plasma gun output, the CAP is ignited and sustained in the whole range of the gas flow rate studied in this research when $U_o > U_b$. It was found that the length of the plasma plume depends on the gas flow by changing it from 2–3 mm at 0.5 l/min to 20–25 mm at 5 l/min. An additional increase in the gas flow rate is not accompanied by the increase in length of the

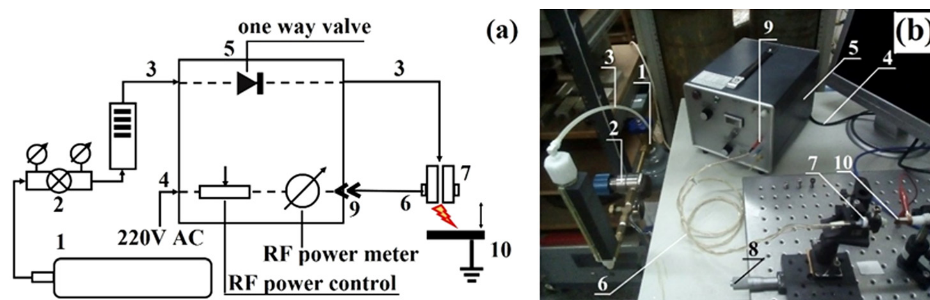

FIG. 4. (a) Apparatus schematic. (b) View of the experimental setup. 1. Gas cylinder. 2. Gas pressure reducer and flow meter. 3. Gas tube. 4. ac power cable; 5. rf generator; 6. rf coaxial cable. 7. Movable plasma gun. 8. Screw to move the plasma gun. 9. Standard BNC rf connector. 10. Plasma target (grounded).

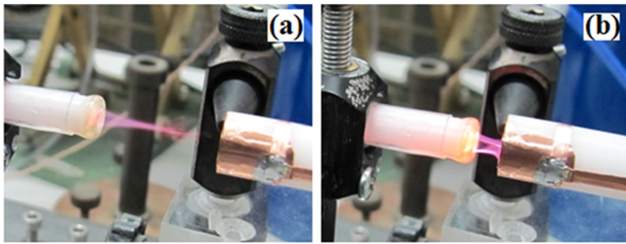

FIG. 5. Images of the plasma plume for different distances d between the grounded target and the output of the plasma gun. (a) $d = 2.3$ cm and (b) $d = 0.4$ cm. Gas flow rate 5 l/min, rf voltage 1150 V, rf pulse repetition rate 178 Hz, rf pulse duration 640 μs.

plasma plume. The latter can be related to the vorticity of the gas flow and its spreading in background air.

Typical images of the plasma plumes for the cases with and without the plume contact with the target are shown in Fig. 5. One can see that for the case when the target is not touched by the plasma plume, the latter has the form of a cone with base diameter equal to the inner diameter of the quartz tube. The images of the plasma plume luminosity were taken by an intensified 4QuikE camera operating with a frame time duration of 20 ns. The obtained images showed that the duration of the light intensity of the plasma plume definitely exceeds the period of the rf voltage ($\sim 0.6\,\mu$s). Also, it was found that the plasma decay weakly depended on the gas flow rate in the range we have studied.

A typical dependence of the power delivered to the plasma on the amplitude of the applied rf voltage U_0 is shown in Fig. 6(a). One can see a linear dependence of the deposited power on the applied voltage allowing estimation of the minimal voltage $U_s \approx 410$ V across the plasma which is necessary to keep the plasma discharge. Here, we note that this value of U_s was found to be almost constant in the whole investigated ranges of pulse duration, repetition rate, and gas flow.

The dependence of the rf power delivered to the plasma on the distance between the output of the plasma gun and the target is shown in Fig. 6(b) for various repetition rates of the rf pulses. One can see that at any fixed distance, the deposited power increases with the increase in the repetition rate. Also, for a fixed repetition rate, one obtains that the power increases versus the distance to the target, i.e., the length of the plasma plume. However, at distances $d \geq 20$ mm when the plasma plume does not touch the target, one obtains $\sim$10 times decrease in the power delivered to the plasma plume.

To compare between the experimental and modeling results, we note that the capacitor C_d (see Fig. 2) connected in series with the plasma load (C_g and R_g) controls the rf current in this electrical circuit. In the experiment, C_d represents the capacitance between the outer ring electrode and the plasma inside the quartz tube which plays the role of an inner electrode. The value of C_d was determined using the Field Precision software package. Considering the experimental geometry presented in Fig. 7, the result of these simulations yields $C_d \leq 2$ pF which satisfactorily agrees with the measurements of this capacitance using RLC meter FLUKE PM6306 which showed C_d in the range 2–3 pF. Here, the plasma was substituted by a metal bar inserted inside the PYREX tube. For further estimates, the value $C_d = 2.5$ pF will be considered. Here, we neglect the capacitance between the ring electrodes and the target (C_g in Fig. 2) which is significantly smaller than the value of C_d. Now, applying in this case Eq. (14), $Q = 0.5\omega C_d U_s\ (U_0^2 - U_s^2)^{1/2}$ with $\omega = 9.42 \times 10^6$ rad/s, $C_d = 2.5$ pF, $U_s = 400$ V and $U_0 = 1150$ V, one obtains for the power dissipated in the plasma plume $Q = 4.7$ W. The latter results in an average rf power of 1.4 W, 0.9 W and 0.47 W for each repetition rate (duty cycle), 450 Hz (0.3), 300 Hz (0.2), and 150 Hz (0.1), respectively, used in our experiments. These results are in a good agreement with the measured values of the power deposited into the plasma plume (see Fig. 6).

When the distance between the plasma gun and the target is increased but remains smaller than 20 mm, the deposited rf power increases as well [see Fig. 6(b)]. This can be explained by the fact that even the longest ($\sim$2.5 cm) plasma plume should be considered as a "short" plume according to the criterion (31) for $C_d = 2.5$ pF and plasma plume diameter $a = 4$ mm. In this case, following Eq. (33), for a short but finite length plasma column, the total dissipated power is proportional to its length L.

A further increase in the value of d above 20 mm results in the decrease of the delivered RF power [see Fig. 6(b)]. This transition occurs when the plasma plume does not touch the grounded target. Thus, in order for the rf current to close its current path, one has to consider the stray capacitance between the plasma plume front and the target. In the equivalent electrical scheme, this stray capacitance appears as C_{st} connected in series with C_d [see Fig. 6(c)]. One can estimate the capacitance C_{st} by applying the specific capacitance $\tilde{c} = 0.5/\ln(L/a)$ used for the derivation of Eq. (26). Indeed, for a plasma column having 2 cm in length and average

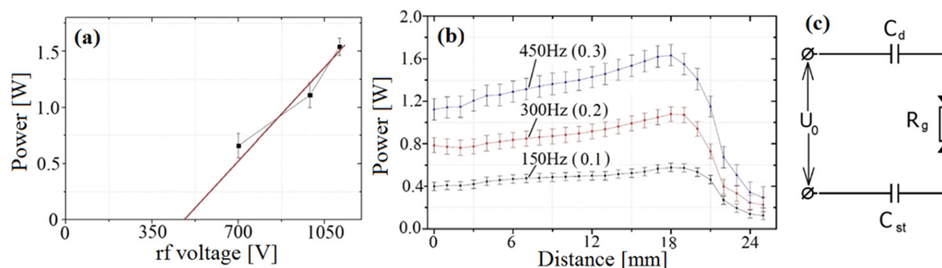

FIG. 6. (a) Dependence of the rf power delivered to the plasma on the amplitude of the rf voltage. Pulse duration 640 μs, repetition rate 300 Hz. (b) Dependence of the rf power delivered to the plasma on the distance between the plasma gun output and the target. Amplitude of rf voltage 1150 V, pulse duration 640 μs, gas flow rate 5 l/min. The duty cycle is indicated in brackets. (c) Equivalent scheme of a plasma plume which does not touch the target. U_0 is the amplitude of the applied rf voltage, C_d and C_{st} are the plasma gun and stray capacitances, respectively, and R_g is the equivalent plasma resistance.

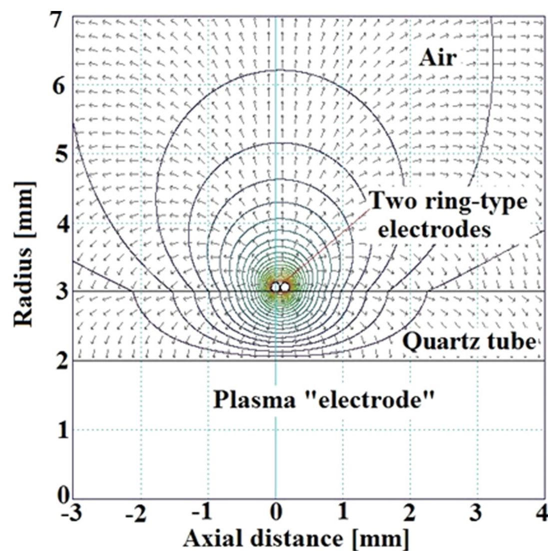

FIG. 7. Equipotential lines and electric field distribution for the capacitor consisting of two ring electrodes: quartz tube as an insulator and plasma as a second electrode.

diameter of ~0.2 cm, one obtains $C_{st} = 0.4$ pF. Such a small capacitance, being included in the equivalent electrical scheme, drastically (about 7 times) reduces the rf current through the plasma and, consequently, the delivered power.

In our experiments, the length of the plasma plume was limited mainly by the turbulence of the gas flow because of its interaction with background air at atmospheric pressure. The typical length, along which this turbulence is developed, is a quite a sophisticated problem and has not been studied yet. Nevertheless, if this turbulence of the gas flow is avoided (e.g., a gas flow in a dielectric tube), the plasma plume, according to Eq. (32), can be as long as tens of cm which agrees with the results obtained in Refs. 17–20. However, placing such a plasma-carrier dielectric tube inside a conducting medium (e.g., a biological object) leads to a significant reduction of the plasma length, i.e. the plasma is almost terminated crossing into the object border [see Eq. (35)].

IV. SUMMARY

In this paper, we present a simple model of DBD discharges. This model describes CAP generated in different experimental conditions, namely different electric field periods as compared with the generated plasma life time, as well as different discharge conditions (plasma plume is free or limited by the target position). The model allows one to estimate the rf power delivered to the CAP plasma, the length of the plasma plume, and the input impedance of the plasma gun versus the applied voltage amplitude, carrier frequency, repetition rate, etc. The results of this model were found to be in a good agreement with the recent experimental studies.

ACKNOWLEDGMENTS

The research was funded by the MAGNET Program, in the Office of the Chief Scientist of the Ministry of Industry, Israel. Grant Nos. # 55254 and #55255; http://www.magnet.org.il/.

[1] J. Winter, R. Brandenburg, and K.-D. Weltmann, Plasma Sources Sci. Technol. **24**, 064001 (2015).
[2] M. G. Kong, B. N. Ganguly, and R. F. Hicks, Plasma Sources Sci. Technol. **21**, 030201 (2012).
[3] A. Schutze, J. Y. Jeong, S. E. Babayan, J. Park, G. S. Selwyn, and R. F. Hicks, IEEE Trans. Plasma Sci. **26**, 1685 (1998).
[4] C. Tendero, C. Tixier, P. Tristant, J. Desmaison, and P. Leprince, Spectrochim. Acta Part B **61**, 2 (2006).
[5] M. Laroussi and T. Akan, Plasma Process. Polym. **4**, 777 (2007).
[6] L. Bárdos and H. Baránková, Thin Solid Films **518**, 6705 (2010).
[7] P. Bruggeman and R. Brandenburg, J. Phys. D: Appl. Phys. **46**, 464001 (2013).
[8] C. Hoffmann, C. Berganza, and J. Zhang, Med. Gas Res. **3**, 21 (2013).
[9] M. Keidar, A. Shashurin, O. Volotskova, M. A. Stepp, P. Srinivasan, A. Sandler, and B. Trink, Phys. Plasmas **20**, 057101 (2013).
[10] E. Robert, M. Vandamme, L. Brullé, S. Lerondel, A. LePape, V. Sarron, D. Riès, T. Darny, S. Dozias, G. Collet, C. Kieda, and J. M. Pouvesle, Clin. Plasma Med. **1**, 8 (2013).
[11] A. Shashurin and M. Keidar, Phys. Plasmas **22**, 122002 (2015).
[12] O. V. Penkov, M. Khadem, W.-S. Lim, and D.-E. Kim, J. Coat. Technol. Res. **12**, 225 (2015).
[13] S. Wu, Y. Cao, and X. Lu, IEEE Trans. Plasma Sci. **44**, 134 (2016).
[14] K.-D. Weltmann and T. von Woedtke, Plasma Phys. Controlled Fusion **59**, 014031 (2017).
[15] A. Fridman and G. Friedman, *Plasma Medicine* (Wiley, New York, 2013).
[16] S. Liu and M. Neiger, J. Phys. D: Appl. Phys. **34**, 1632 (2001).
[17] Z. Hong-Yan, W. De-Zhen, and W. Xiao-Gang, Chin. Phys. **16**, 1089 (2007).
[18] Z. Xiong and M. J. Kushner, Plasma Sources Sci. Technol. **21**, 034001 (2012).
[19] Z. Xiong, E. Robert, V. Sarron, J.-M. Pouvesle, and M. J. Kushner, J. Phys. D: Appl. Phys. **45**, 275201 (2012).
[20] D. Breden, K. Miki, and L. L. Raja, Plasma Sources Sci. Technol. **21**, 034011 (2012).
[21] Y. Binenbaum, G. Ben-David, Z. Gill, Y. Z. Slutsker, M. A. Ryzhkov, J. Felsteiner, Y. E. Krasik, and J. T. Cohen, PLoS One **12**(1), e0169457 (2017); R. Shtrichman, Y. Binenbaum, Y. D. La Zerda, G. Ben-David, G. Ziv, Y. Z. Slutsker, M. A. Ryzhkov, J. Felsteiner, Y. E. Krasik, and J. T. Cohen, in Abstract Book of 4th International Workshop on Plasma for Cancer Treatment (Institute Curie, 27–28 March, Paris, France).
[22] Y. P. Raizer, *Gas Discharge Physics* (Springer-Verlag, Berlin, Heidelberg, 1991).
[23] U. Kogelschatz, Plasma Chem. Plasma Process. **23**, 1 (2003).
[24] T. C. Manley, J. Electrochem. Soc. **84**, 83 (1943).
[25] V. B. Gil'denburg, Sov. Phys. JETP **51**, 480 (1980).
[26] E. Karakas, M. A. Akman, and M. Laroussi, Plasma Sources Sci. Technol. **21**, 034016 (2012).
[27] X. P. Lu and M. Laroussi, J. Appl. Phys. **100**, 063302 (2006).
[28] X. Lu, G. V. Naidis, M. Laroussi, and K. Ostrikov, Phys. Rep. **540**, 123 (2014), and references therein.
[29] Y. Akishev, G. Aponin, A. Balakirev, M. Grushin, V. Karalnik, A. Petryakov, and N. Trushkin, Plasma Sources Sci. Technol. **22**, 015004 (2013).
[30] M. Moisan, C. M. Ferreira, Y. Hajlaoui, D. Henry, J. Hubert, R. Pantel, A. Ricard, and Z. Zakrzewski, Rev. Phys. Appl. **17**, 707 (1982).